ANNALI DI GEOFISICA, VOL. 42, N. 6, December 1999

Global Seismic Hazard Assessment Program (GSHAP) in continental Asia

Peizhen Zhang ([1]), **Zhi-xian Yang** ([2]), **Harsh K. Gupta** ([3]), **Satish C. Bhatia** ([3]) **and Kaye M. Shedlock** ([4])
([1]) *Institute of Geology, China Seismological Bureau, Beijing, China*
([2]) *Institute of Crustal Dynamics, China Seismological Bureau, Beijing, China*
([3]) *National Institute of Geophysics, Hyderabad, India*
([4]) *USGS, Golden, CO, U.S.A.*

Abstract
The regional hazard mapping for the whole Eastern Asia was coordinated by the SSB Regional Centre in Beijing, originating from the expansion of the test area initially established in the border region of China-India-Nepal-Myanmar-Bangla Dash, in coordination with the other Regional Centres (JIPE, Moscow, and AGSO, Canberra) and with the direct assistance of the USGS. All Eastern Asian countries have participated directly in this regional effort, with the addition of Japan, for which an existing national hazard map was incorporated. The regional hazard depicts the expected peak ground acceleration with 10% exceedance probability in 50 years.

Key words *seismic hazard assessment – continental Asia – historical earthquakes – China – UN/IDNDR*

1. Introduction

Continental Asia is a region with a high level of seismic hazard (Gu, 1983; Ma *et al.*, 1989; Gupta, 1993; Zhang, 1993). Earthquakes in continental Asia have caused widespread loss of life, property damage, and social and economic disruption. For example, the nine $M_S \geq 7$ earthquakes that successively struck China from 1966 to 1978 (Ma *et al.*, 1989) are tragic examples of seismic disasters in continental Asia. Several of these earthquakes occurred in densely populated areas and resulted in approximately 300 000 casualties. Major earthquakes in Japan, India, Burma, and other countries in continental Asia also have caused great loss of life and economic disaster. Thus, seismic hazards pose a major threat to the social and economic development of most countries in continental Asia, most of which are developing nations.

The most effective way to reduce disasters caused by earthquakes is to estimate the seismic hazard and disseminate this information for use in improved building design and construction. Seismic hazard estimates, however, are not available for many countries in continental Asia. GSHAP intends to fill this critical gap and increase the ability of each country to assess its seismic hazard. The primary goal of GSHAP is to ensure that national agencies are able to assess seismic hazard in a regionally coordinated fashion using advanced methods (Giardini and Basham, 1993). Thus, GSHAP is intended as a global effort to be conducted at the regional level, based on the establishment of Regional Centers where data will be assembled and analyzed on national and regional scales. Beijing is the regional center for Central and Southern Asia. Countries that work with the Beijing Regional Center include India, Nepal, Bangladesh,

Mailing address: Dr. Peizhen Zhang, Institute of Geology, China Seismological Bureau, Beijing 100029, China; e-mail: peizhen@public3.bta.net.cn

Bhutan, Myanmar, Thailand, Laos, Vietnam, Cambodia, Malaysia, Singapore, Sri Lanka, South Korea, North Korea, Mongolia, Japan, Kazakhstan, Tadzhikhstan, Kirghizstan, and China (fig. 1).

The realistic assessment of seismic hazard can not be limited to data and information available within national boundaries, especially for countries that share seismotectonic structures or seismic zones. Information available across the neighboring national boundaries has to be used. To date, however, this has not been the case in most studies of seismic hazard assessment in the world. That in turn causes significant uncertainties in seismic hazard assessment and sometimes creates contradictions across national boundaries. Concatenation of available national seismic hazard maps from China, India, Bangladesh, Myanmar, and Vietnam illustrates the problems (fig. 2). First, there are gaps in Bhutan, Nepal, Vietnam and Laos, which do not have national seismic hazard maps. Second, mismatches occur along most national boundaries. For example, along the China-Myanmar boundary, the expected earthquake intensity in 50 years is VII on China side, but is IX across the border in Myanmar. In India, the seismic hazard is given by peak ground acceleration, but in neighboring countries such as China and Myanmar the hazard is given in intensity grades. These inconsistencies are due to incomplete datasets and inconsistent methods of hazard estimation. Each country used only their own data to assess seismic hazard even when significant, damaging earthquakes occurred in neighboring countries. GSHAP hopes to rectify these problems by assessing seismic hazard in a regionally coordinated fashion.

Fig. 1. Map of countries that cooperated in the continental Asia GSHAP effort. Box outlines the Test Area of the first phase of GSHAP implementation in the region.

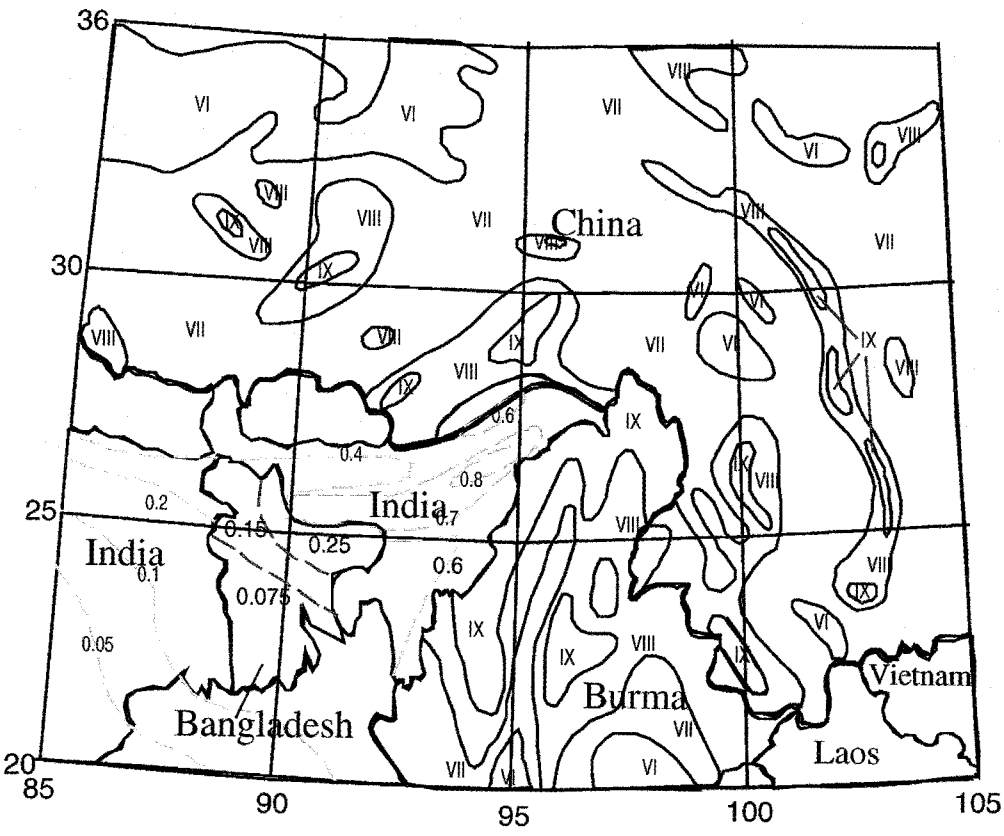

Fig. 2. Pre-GSHAP status of seismic hazard assessment in the Test Area (see fig. 1). This map is the concatenation of existing national seismic hazard maps. The values shown for India are expected peak ground acceleration (g) while all other countries depict expected peak seismic intensities in 50 years.

2. GSHAP activities

The First Workshop on Implementation of GSHAP in continental Asia was held in Beijing in 1994. Participants included representatives from most countries in the region. During that workshop we formulated technical guidelines for the implementation of GSHAP in the region, and we finalized the test area (fig. 1) for the first phase of seismic hazard assessment studies. A Proceeding of this workshop was published in 1995 (Zhang, 1995). The test area is located in the boundary region (20°-35°N, 85°-105°E) of China, India, Myanmar (Burma), Bangladesh, Nepal and Vietnam (fig. 1). In early 1996, a second workshop was hold in Hyderabad, India. During this workshop we merged existing earthquake catalogs, discussed seismic source zoning, and learned how to use a common suite of software to calculate seismic hazard for the test area. The seismic hazard assessment results from the Test Area were presented at the Regional Assembly of the IASPEI at Tangshan, China in August 1996 (Yang and Zhang, 1996; Zhang and Yang, 1996). Following the GSHAP strategy, the methods applied to the test area were applied to the whole of continental Asia. Preliminary results were presented in 1997 during the IASPEI General Assembly in Thessaloniki,

Greece (Bhatia *et al.*, 1997; Yang, 1997; Zhang and Yang 1997) and at a GSHAP workshop in Golden, CO, U.S.A., in 1998.

3. Nature of seismic hazard in Central and Southern Asia

Late Quaternary deformation of continental Asia is distributed over a vast region, and includes a full spectrum of deformational styles and structural orientations. Much, if not all, of the deformation can be attributed to the collision and subsequent penetration of the Indian plate with respect to Eurasia (for example, Molnar and Tapponnier, 1975, 1978; Tapponnier and Molnar, 1977, 1979). The occurrence and distribution of strong earthquakes are the manifestation and result of this deformation. The locations of earthquakes, especially large earthquakes, are not uniformly and randomly distributed – rather they cluster in belts and regions of prominent late Quaternary tectonic activity (Tapponnier and Molnar, 1977; Molnar and Deng, 1984).

3.1. *Himalayan frontal arc*

Intense seismic activity associated with the Himalayan frontal arc effects India, Nepal and

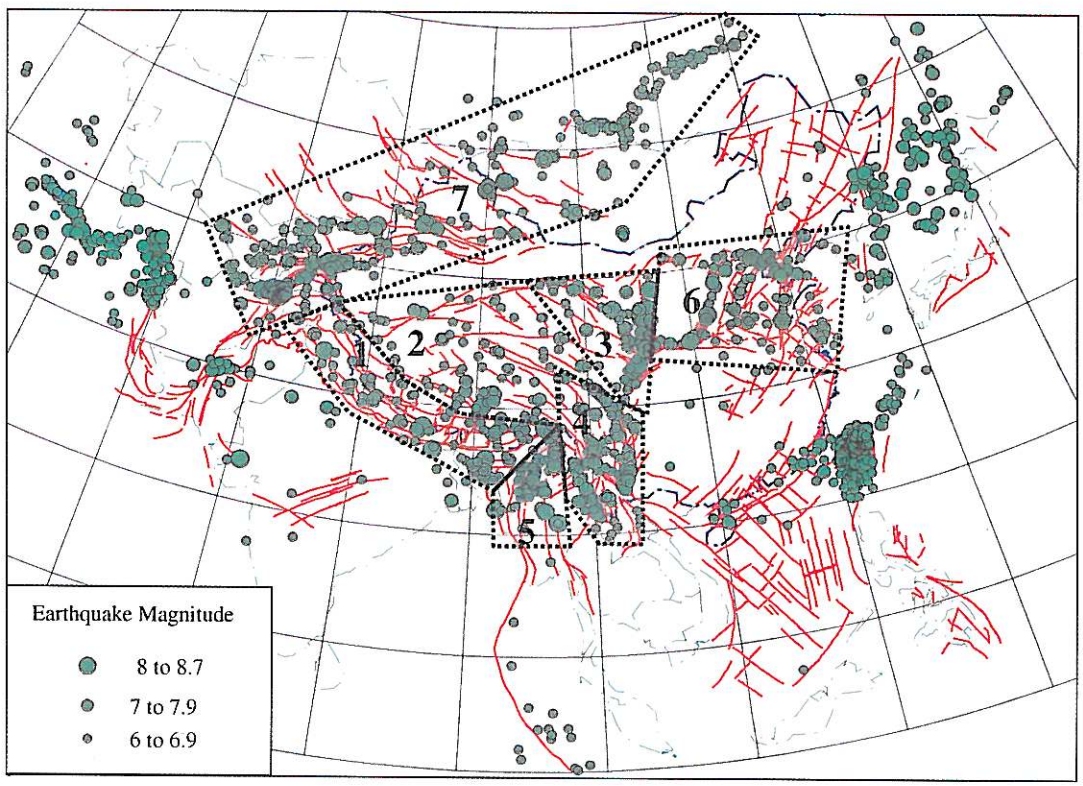

Fig. 3. Seismotectonic map of continental Asia. Thick lines are active faults. Solid dots are earthquakes with $M_s \geq 6.0$. Lightly shaded areas are the regions discussed in the text. 1) Is the Himalayan frontal arc region; 2) is the Tibetan plateau region; 3) is the northern and eastern margins of the Tibetan plateau; 4) is the Yunnan and Sichuan region; 5) is the Myanmar (Burma) region; 6) is the Northern China region, and 7) is the Pamir - Tianshan - Mongolia region.

Bangladesh. The approximately 2000 km long Himalayan frontal arc (from the western syntaxis in Kashmir to the eastern syntaxis in Assam) has been very active seismically (fig. 3). More than a dozen earthquakes of $M_S > 7.5$ have occurred in this region since 1897 (Gupta, 1993). The seismic activity in the Himalayan frontal arc is the result of continued collision between the Indian and Eurasian plates (Molnar and Tapponnier, 1975; Tapponnier and Molnar, 1977; Curry *et al.*, 1979; Le Dain *et al.*, 1984; Gupta and Bhatia, 1986). Three fault zones dominate the deformation of the Himalayan frontal arc: the Main Central Thrust (MCT), the Main Boundary Thrust (MBT), and the Frontal Thrust. It appears that tectonic activity has been shifting from the MCT and MBT in the north to the Frontal Thrust in the south, along which the Indian sub-continent underthrusts beneath the Himalayas (Molnar and Lyon-Caen, 1989).

The 2000 km long Himalayan frontal arc experienced four great earthquakes ($M_S > 8$) in the short span of 53 years (Gupta, 1993): the Shillong earthquake of 1897; the Kangra earthquake of 1905; the Bihar-Nepal earthquake of 1934; and the Assam-Chayu earthquake of 1950. These four earthquakes may have ruptured 1400 km of the frontal arc. The remaining 600-km of the Himalayan frontal arc was partially, or possibly totally, ruptured by large ($M_S \geq 7$) earthquakes in 1803 and 1833. The extent of rupture associated with these two earthquakes is poorly constrained. If these two earthquakes did not rupture the entire 600 km, then the unruptured portion must be considered likely to rupture in the near future, possibly in a great earthquake. Repeat time for an earthquake of $M_S \geq 8$ is estimated to be 200 to 270 years, and the amount of time required for the entire Himalayan frontal arc to be ruptured in a series of large or great earthquakes is between 180 and 240 years (Seeber and Ambruster, 1981).

3.2. *Tibetan plateau*

Although many great earthquakes have occurred along the margins of the Tibetan plateau, the world's highest plateau itself is also has experienced great earthquakes. More than 30 $M_S > 7$ earthquakes have occurred in the interior of the Tibetan plateau, and five of them are $M_S \geq 8$ (Gu, 1983; Ma, 1989).

Fault plane solutions of 23 well constrained earthquakes show normal and strike-slip mechanisms with consistent T-axes oriented between east-west and northwest-southeast (Ni and York, 1978; Chen and Molnar, 1983; Molnar and Lyon-Caen, 1989). There appears to be geographic variation in the style of faulting. Earthquakes that occurred closest to the highest Himalayas show nearly pure normal faulting, but further north, strike-slip and normal faulting seem to be equally common (Molnar and Lyon-Caen, 1989). Active fault studies in the Central Tibetan plateau also reveal this pattern of normal and strike-slip faulting (Armijo *et al.*, 1986; Wu *et al.*, 1992). The southern part of the Tibetan plateau is characterized by a series of north-south trending grabens. Surface ruptures associated with major earthquakes often occur along boundaries of these active grabens. For example, the 1952 Dangxiong, Tibet, earthquake was associated with a 57-km long surface rupture zone along the basin boundary. The maximum displacement was 5.5 m and the horizontal offset was 3.6 m (Wu *et al.*, 1992).

3.3. *Northern and eastern margin of the Tibetan plateau*

Crustal shortening is the predominant late Cenozoic tectonic process in this area as the Tibetan plateau is apparently being overthrust to the north and to the east, with much of this deformation accommodated by several prominent left-lateral strike-slip faults such as the Altyn Tagh and Haiyuan faults (Peltzer and Tapponnier, 1988; Institute of Geology, 1993). Mapped active reverse faults and reverse faults with a strong strike-slip component dominate this belt of deformation. Fault plane solutions of earthquakes also show thrust faulting with strike-slip component (Molnar and Lyon-Caen, 1989).

Four earthquakes of $M_S > 7$ have occurred in this region during the twentieth century. Each of the earthquakes was associated with surface ruptures of over 100 km in length (Zhang *et al.*, 1987; Peltzer and Tapponnier, 1988; Institute of

Geology, 1993). The 1920 Haiyuan earthquake caused 220 000 deaths and destroyed thousands of towns and villages (Zhang *et al.*, 1987). This earthquake had M_S = 8.6 and created about 300 km of surface rupturing (Zhang *et al.*, 1987). Only seven years after the Haiyuan earthquake, an earthquake of M_S = 7.9 (the Gulang earthquake) occurred less than 100 km west of the Haiyuan surface rupture zone. This earthquake also resulted in significant casualties and economic losses (Lanzhou Institute of Seismology and Ningxia Seismological Bureau, 1982).

3.4. *Yunnan - Sichuan*

Yunnan - Sichuan is another seismically active region. There have been 32 earthquakes with $M_S > 7$ since the beginning of documented history in the region 1500 years ago (Gu, 1983; Ma, 1989). Two events among them have $M_S > 8$. These earthquakes caused a great number of casualties and significant economic damage.

Earthquakes in this region are characterized by shallow strike-slip faulting (focal depths between 10 and 15 km; Zhou *et al.*, 1983; Allen *et al.*, 1989). The seismicity of the region may be divided into two sub-regions, the Western Sichuan - Eastern Yunnan sub-region and the Western Yunnan sub-region (fig. 3). Earthquakes in the Western Sichuan - Eastern Yunnan subregion occur mainly in the northwestern trending Xianshuihe and the north-trending Xiaojiang fault systems. The Xianshuihe fault is a 450 km long left-lateral strike-slip fault with a Holocene slip rate of 13 mm/yr. Nine earthquakes with $M_S > 7$ have occurred along this fault zone. The latest one, the 1973 Luhuo earthquake (M_S = 7.9) was associated with 90 km of surface rupture and a maximum left-lateral displacement of 6 m (Tang *et al.*, 1984). To the south, the Xianshuihe fault, which curves into the north-south trending Xiaojiang fault, also is a source of strong earthquakes. For example, the 1833 Songming earthquake (M_s = 8) occurred along this fault.

Earthquakes are widely distributed in the Western Yunnan seismic sub-region. Both major active faults with lengths of several hundred kilometers (*i.e.* the Red River and Jingsha Jiang faults), and short faults with different orientations host occurrences of strong earthquakes in the Western Yunnan sub-region (fig. 3). The frequency of occurrence of earthquakes in this sub-region is the highest within China. This very active seismic sub-region is part of the Assam - Yunnan - Myanmar earthquake region resulting from the penetration of the Indian plate into the Eurasian plate (Molnar and Tapponnier, 1975; Tapponnier and Molnar, 1977; Tapponnier *et al.*, 1982; Le Dain *et al.*, 1984; Gupta, 1993).

3.5. *Myanmar (Burma) region*

Seismotectonic processes in the Myanmar region are very complex (Le Dain *et al.*, 1984). This region accommodates the large strike-slip movement of India with respect to Southeast Asia (Le Dain *et al.*, 1984; Gupta and Bhatia, 1986, 1993). At least nineteen earthquakes of $M_S > 7$ have occurred in the region. The great Arakan earthquake of 1762 caused extensive changes in the level of the Myanmar (Burma) coast (Richter, 1958). The 1878 earthquake caused uplift of 6 m on the west coast of Ramree island, while another island seems to have disappeared (Richter, 1958). Another event in 1843 was associated with the eruption of mud volcanoes.

3.6. *North China region*

The North China basin is an extensional region of high seismic hazard. Strike-slip and normal faults are the predominant active structures in the North China region (fig. 3). The regional extension is probably caused, in part, by southeastward extrusion of Southeastern Asia with respect to Eurasia (Tapponnier and Molnar, 1977; Peltzer and Tapponnier, 1988). There have been 6 earthquakes of $M_S \geq 8$ and 16 earthquakes of $M_S \geq 7$ in this region during the past 2000 years (Gu, 1983; Ma, 1989). These large earthquakes generally have occurred along major active faults that bound large basins. Fault-

plane solutions of these earthquakes are commonly right-lateral strike-slip with a normal dip-slip component.

Although earthquake recurrence intervals along any individual fault are relatively long (usually in the range of several thousand years), the composite recurrence interval for the whole region is on the order of a few decades (Ma *et al.*, 1989). The region is densely populated, and is the cultural and economic center of China. Every earthquake of $M_S \geq 6$ has the potential for causing serious loss of life and economic damage (Ma *et al.*, 1989). Five earthquakes with $M_S > 7$ occurred in this region within the decade between 1966 and 1976. These earthquakes resulted in hundreds of thousands of casualties and significant economic damages. The 1976 Tangshan earthquake is a tragic example of the nature of seismic hazard in this region. During this earthquake, 240 000 people were killed and direct economic losses reached approximate $ 1 billion RMB.

3.7. *Pamir - Tianshan - Mongolia*

This seismic belt is situated in the interior of continental Asia (fig. 3). The Pamir plateau is one of the most seismically active regions in the world. Many earthquakes with $M_S > 7$ have occurred in the Pamir during the twentieth century. A zone of intermediate earthquakes dips south-southeast beneath the Pamir. This is generally taken as evidence for subduction of the cold Tianshan lithosphere beneath the Pamir (Burtman and Molnar, 1993).

Late Quaternary deformation in the Tianshan mountain is dominated by reverse faulting and crustal shortening and associated conjugate strike-slip faulting north of the Tianshan. The structural convergence in the Tianshan is also attributed to India's penetration into Eurasia (Nelson *et al.*, 1987; Avouac *et al.*, 1993; Baljinnyam *et al.*, 1993). Neotectonics in Mongolia is characterized by strike-slip faulting with thrust dip-slip components. The 1955 Gobi Altai ($M_S = 8$) earthquake was associated with 8 m left-lateral displacement and about 5 m vertical offset (Tapponnier and Molnar, 1979; Molnar and Deng, 1984; Baljinnyam *et al.*, 1993). Lake Baikal is part of an intracontinental rift system, characterized by normal faulting and crustal extension. There have been nine earthquakes of $M_S \geq 8$ and 22 earthquakes of $M_S \geq 7$ in the Tianshan-Mongolia-Lake Baikal seismic belt. Fault plane solutions of these earthquakes indicate east-trending reverse faulting in the Tianshan, strike-slip faulting in Mongolia, and normal faulting in the Lake Baikal region, consistent with results of late Quaternary deformation in this belt (Chen and Molnar, 1983; Tapponnier and Molnar, 1979; Molnar and Deng, 1984; Nelson *et al.*, 1987).

4. Current status in national seismic hazard assessment

Seismic hazard assessment is a fundamental step toward reduction of the effects of seismic hazards. Seismic hazard assessments serve as the basis for introducing low-cost earthquake-resistant building design and construction. Although Central and Southern Asia is a region with a high level of seismic hazard, seismic hazard assessments have not been performed in every country. We review the existing seismic hazard assessments of the countries in the GSHAP test area.

4.1. *China*

The work of national seismic hazard assessment conducted in China, in conjunction with the U.S.S.R., began in the early 1950's. These early assessments were guided by two important principles proposed by the Russian seismologist Gorshkov: 1) earthquakes of similar magnitude will recur where they have previously, and 2) regions of similar tectonic structure are subject to similar seismic potential. Both China and the former U.S.S.R. compiled their first national seismic hazard maps in the early 1950s based on these two principles. In 1977, China finished a second version of its national seismic hazard map based on available seismic and seismotectonic data, and the predicted maximum seismic intensity for the time period of one hundred years (State Seismological Bureau,

1981). This map was used to develop a new national building code for China.

In 1992, China published its third national seismic hazard map (State Seismological Bureau, 1992). With the 1992 map, China began using the Cornell (1968) probabilistic approach of seismic hazard analysis instead of the deterministic approach utilized in the previous two versions. The 1992 map depicts intensities with an exceedance probability of 10% for a period of 50 years given average site conditions (Shi and Gao, 1991; State Seismological Bureau, 1992).

Earthquake activity in China varies temporally and spatially. In order to incorporate this variability, Liu (1987) suggested a two-level delineation of seismic source zones be used in the national seismic hazard map of China (State Seismological Bureau, 1992). The first level of seismic source zone delineation is a seismic belt (or seismic region). The size of a seismic belt is determined by the availability adequate earthquake data for statistical analysis. The second level of seismic source zone delineation is a seismic source. This level of delineation incorporates the spatial variability of the earthquake distribution through weights assigned to each seismic source within a seismic belt. The weights for each source are calculated to sum to the total probability of earthquake recurrence within the larger seismic belt.

A new national seismic hazard map of China based on the two-level delineation of seismic sources has just been completed by State Seismological Bureau. The seismic hazard in the new map is depicted as Peak Ground Acceleration (PGA) instead of intensity grades.

4.2. *India*

The first national seismic hazard map of India was compiled by the Geological Survey of India in 1935 (Krishina, 1992). A second national seismic hazard map was published in 1965, based primarily on earthquake epicentral and isoseismal maps published by the Geological Survey of India. Epicenters of earthquakes with $M_s \geq 5$ were mapped. Modified Mercalli intensity isoseismals (ranging from V to IX) from some strong earthquakes were superimposed on the epicenter map to determine the seismic zones. Minor modifications were made to account for local effects such as those indicated along the Aravally axis by the Delhi earthquake (Krishina, 1992).

As knowledge of earthquakes increased, two revisions of the national hazard maps were made in 1966 and 1970, respectively (Krishina, 1992). The revised maps more closely represented known seismotectonic features without sacrificing the information obtained from earthquakes and from theoretical ground motion attenuation relationships. Another significant change in the revised maps was the abolition of zone zero, in recognition of the fact that it was not scientifically sound to depict any region of India to have the probability of an earthquake equal to zero. This had the desired effect of including some level of seismic provisions in the design of important structures (Krishina, 1992).

Khattri (1992) prepared a probabilistic seismic hazard map of the Himalayas and adjoining areas that depicts contours of peak acceleration (in % g) with a 10% probability of exceedance in 50 years. The conventional Cornell (1968) probabilistic method was used to produce the 1992 map.

4.3. *Bangladesh*

The first seismic hazard map for Bangladesh was compiled by the Geological Survey of India in 1935. The northern part of Bangladesh was designated to be «liable to severe earthquake damage» (Ali and Choudhury, 1994). In the sixties, the meteorological department prepared a hazard map that was adopted by the Bangladesh Meteorological Department in 1972. The country was divided into four zones: major damage (10%-20% g), moderate damage (6.7%-10% g), minor damage (5%-6.7% g) and negligible damage (< 5% g) (Ali and Choudhury, 1994). The map was revised in 1979. An outline of a code for earthquake resistant design was also prepared (Geological Survey of Bangladesh, 1979). This map and outline have formed the basis for design of most of the important structures built during the last 15 years.

In 1992, the Government appointed a team of consultants to prepare a National Building Code for Bangladesh. As part of this study, a comprehensive review of present data has been undertaken and a revised seismic hazard map has been compiled (Ali and Choudhury, 1994). The results have been incorporated in the Bangladesh National Building Code. The hazard map retains the major features of the earlier maps and divides the country into three zones. The zone of highest hazard includes the north and northeastern parts, based on surface acceleration contours $\geq 0.2\ g$ for a 200-year return period.

4.4. *Myanmar (Burma)*

Myanmar has suffered from more than 20 large earthquakes during the last 200 years (Swe, 1994). Seismic monitoring and seismic zoning in Myanmar is in the beginning stage. There are four seismic stations in Myanmar and more are planned in the near future. The transition to a market-oriented economy and rapid development are underway. Thus, there is a pressing need to prepare national seismic hazard maps for earthquake-resistant building design and construction. The current seismic hazard map of Myanmar is based on historical seismicity (Swe, 1994).

4.5. *Vietnam*

Many earthquakes with intensity VII, VIII, and IX (MM, MSK-64 scale) have occurred in Vietnam. These earthquakes have caused some human casualties and great economic loses (Xuyen, 1994). Scientists in Vietnam have taken the following steps to assess seismic hazard: collection and cataloging of earthquake information; compiling seismogenic zone and maximum shaking intensity maps; and assessment of the recurrence period of large earthquakes (Xuyen, 1994). A preliminary hazard map of maximum shaking intensity has been compiled based on the information assembled to date (fig. 7 in Xuyen, 1994).

4.6. *Japan*

Japan long has been a leader in the detection, monitoring, and reporting of earthquakes. The vibrant and active earthquake research community in Japan has produced hundreds of seismic hazard maps throughout recorded history. Japan has no single systematic national program to produce an official seismic hazard map. Instead various agencies produce hazard maps on an 'as needed' basis.

4.7. *Other countries*

There are no official, published seismic hazard maps for remainder of the countries in the GSHAP test area. The earthquake catalogs and seismotectonic information for these countries were obtained from international agencies and publications.

5. Earthquake catalog assembly

Following GSHAP technical guidelines, we have compiled an earthquake catalog for continental Asia bounded by 0°-60°N and 40°-160°E, excluding Japan and the Philippines. The catalog includes Mongolia, Kazakhstan, Tadzhikhstan, Kirghizstan, Korea, India, Myanmar (Burma), Vietnam, Nepal, Pakistan, Laos, Bangladesh, China and other countries (regions). The catalog contains 14 302 events with moment magnitude $\boldsymbol{M} > 5$ (for the mainland of China $\boldsymbol{M} > 4.75$) between 7670 B.C. and 1996: 2287 from the Russian catalog, 3817 from the Chinese catalog, 1680 from the Taiwan area catalog, and 6518 from the PDE and NGDC databases. Distribution of these events in the eras of historical, early instrumental, and modern instrumental is as in table I.

Most of the countries in the region have their own local catalogs. The local catalogs that we used include the Chinese (Gu, 1983; Xie *et al.*, 1989; Min, 1995; Yang, 1997), Indian (Gupta and Bhatia, 1986; Umesh, 1992; Krishina, 1992), Bangladesh (Ali and Chouldhury, 1994), Myanmar (Le Dain *et al.*, 1984), Vietnam (Xuyen, 1994), Russian (Ulomov, 1999), and Taiwan Area (Cheng, unpublished catalog) .

Table I. Number of earthquakes in the regional catalogs.

Time period	Total number	Russia	China	Taiwan area	Others
Pre-1900	1489	382	994	1	112
1901-1963	3432	1032	1286	862	252
After 1964	9381	873	1537	817	6154
	14302	2287	3817	1680	6518

Seismic hazard assessment requires as complete a history as possible of earthquakes in or near the region of interest. It is necessary to have a comprehensive knowledge of historical recording coverage in order to assess the completeness level of an earthquake catalog.

The history of earthquake records differs from one country to another, and even from one seismic zone to another. The earliest Chinese earthquake records can be traced back to 2300 B.C. (Min, 1995). However, the completeness level for earthquakes $M_S > 5$ is only about five hundred years for eastern and three hundred years for Western China. Geographic variation in the completeness level of earthquake catalogs also exists between different seismic zones within China. For example, in the Shanxi seismic zone in Eastern China, the history of earthquakes can be traced back to 780 B.C. Ten strong earthquakes with intensity $\geq$ IX occurred in this zone prior to the 20th century. The highest intensity, XI, is recorded for an earthquake that occurred in 1303. However, the level of seismicity appears to be relatively low during the 20th century, since no earthquake with $M_S \geq 7$ has occurred in this seismic zone. On the contrary, in the Xianshuihe seismic zone in Western China, there have been four earthquakes with $M_S \geq 7$ and fourteen with $M_S \geq 6$ during this century. But the history of earthquakes in the Xianshuihe seismic zone can be traced back only to the early 18th century (1733), about 260 years. The distribution of earthquakes does not exhibit spatial or temporal uniformity anywhere in China. These uncertainties in both the spatial and temporal recurrence of earthquakes must be incorporated into seismic hazard assessments.

The use of a uniform magnitude scale is very important in seismic hazard assessment, as well as in earthquake prediction, seismotectonics, and other seismological research. The moment magnitude ($\boldsymbol{M}$) scale (Hanks and Kanamori, 1979), which measures the size of an earthquake without saturating, has been widely adopted. The GSHAP cooperators agreed to estimate and report the moment magnitudes of all earthquakes in the catalogs (Giardini and Basham, 1993; Giardini and Zhang, 1994). However, other magnitude scales have been used in existing catalogs for a long time, because direct measurement of seismic moment became possible in just the last few decades.

There are four types of magnitude scales in the catalogs from the test area: intensity, Gutenberg surface-wave magnitude (M_S), Beijing surface-wave magnitude, and body-wave magnitude (m_b) scales. We converted them into moment magnitudes using the following scheme:

– Convert different intensity and magnitude scales into IASPEI surface wave magnitude through local empirical relationships.

– Convert IASPEI surface wave magnitude into seismic moment using the relationship established by Ekström and Dziewonski (1988).

– Convert seismic moment into moment magnitude through the definition given by Hanks and Kanamori (1979).

The conversion procedures are diagrammed in fig. 4. A detailed description and discussion of our procedure is given by Yang (1997).

The intensity-based magnitudes of historic (pre 1900) earthquakes reported in the various Asian catalogs were converted to M_S using an empirical formula (Min, 1995)

$$M_S = 0.605\, I_0 + 1.376$$

where I_0 is the macroseismic intensity (Modified Mercalli Scale).

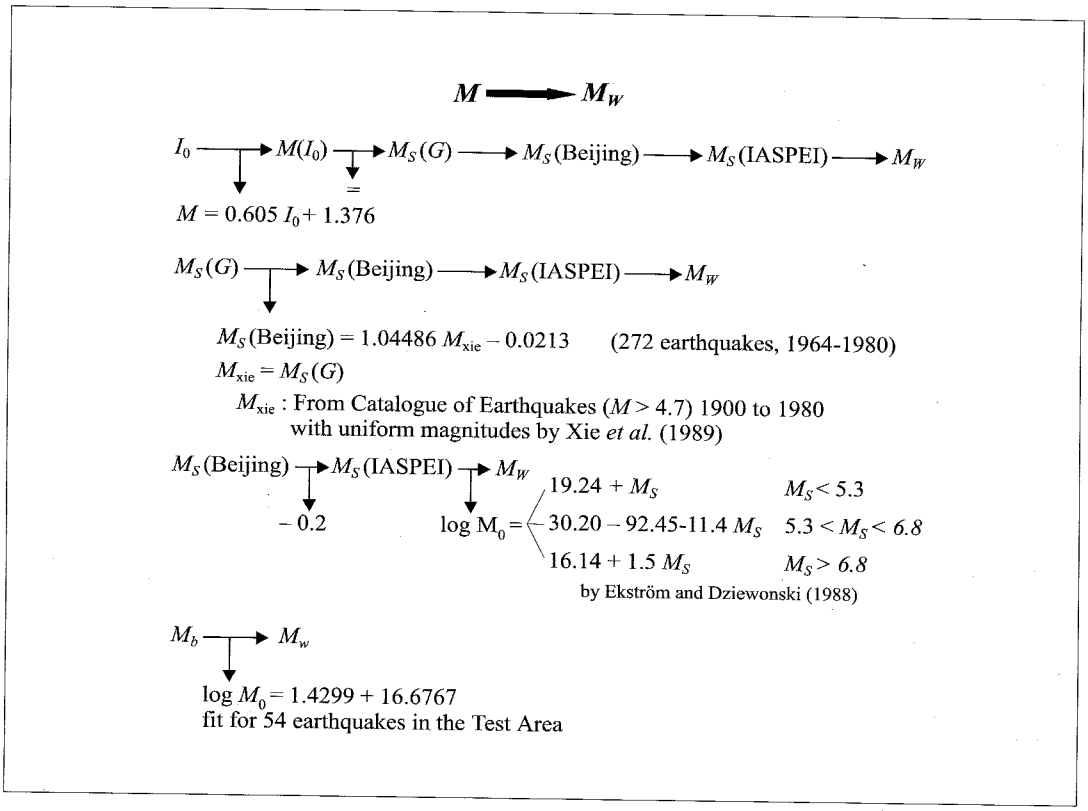

Fig. 4. Steps in magnitude conversion.

Earthquakes recorded during the early instrumental era (1900-1963) are reported with M_S magnitudes in the Chinese, Indian, and Bangladesh catalogs.

The modern instrumental era (post 1963) ushered in an era of somewhat more consistent magnitudes, although differences still exist. In China, earthquakes were reported with Beijing surface-wave magnitudes. A second magnitude began appearing in the China catalog in 1991, «M_S 7». This is a long period surface-wave magnitude determined by records from «seismographer 763» (Institute of Geophysics, SSB, 1991). Magnitude «M_S 7» is very similar to the IASPEI surface-wave magnitude scale (their calibration functions are equal). Beginning with 1998, the Chinese catalog dropped the Beijing surface-wave magnitudes and began reporting only «M_S 7» magnitudes. The Taiwan region catalog reports IASPEI surface-wave magnitudes for earthquakes with $M_S \geq 6$ and a local magnitude scale ($M_L(s)$) for earthquakes with magnitude < 6. The Vietnamese use the formula

$$M_S = 2.67 \log (F - P) - 2.49 + D$$

where $(F - P)$ is duration, and D is a station correction. The PDE and other international agencies report IASPEI surface-wave magnitudes.

We converted the various reported magnitudes into moment magnitude for all earthquakes in the test area catalog. Two major problems prevented us from using the multi-step method described above to convert the various magnitudes into moment magnitude for all of conti-

nental Asia. First, the available data are inadequate to establish robust relationships between different magnitude scales, such as surface-wave magnitude *versus* moment magnitude and body-wave magnitude *versus* seismic moment. Second, some magnitude data provided by local catalogs already are converted values rather than directly measured values. For example, the local catalog for the Taiwan region reports all earthquakes using a local magnitude scale, $M_L(s)$. Many of these $M_L(s)$ values have been calculated from other directly measured or estimated magnitudes, using various conversion functions. Errors in magnitude estimation increase with each scale conversion, in part because the dispersion associated with each relationship is large. Any multi-step conversion scheme may result in final magnitude values that are non-uniform and have large associated errors. Furthermore, for most earthquakes, $M_S \approx \boldsymbol{M}$ (see Chapter 1, Lay and Wallace, 1995). So we used the reported M_S magnitude values in our seismic hazard assessment of Asia.

Another necessary task in the compilation of an earthquake catalog is the removal of duplicate records from different sources. First, all local origin and phase times in the catalogs were corrected to GMT. Then, we compared the catalogs in pairs, using a computer program to select and print all records with differences in origin time less than two minutes. We examined these printed records manually. If there was a local catalog available, we assumed the parameters given by the local catalog for that event. If no local records were available, we selected the parameters from international catalogs such as the ISC.

6. Seismic source zone delineation

Delineation of seismic source zones is a fundamental step in probabilistic earthquake hazard analysis. Seismic source zones are defined as areas that share common seismological, tectonic, and geological attributes under the assumption that these areas also share seismotectonic origins of seismicity that can be described by an unique magnitude-frequency relationship (Thenhaus, 1986). This definition implies that seismicity in a seismic source zone is uniformly distributed throughout the zone and future earthquakes may occur anywhere in the zone. Results from seismicity and paleoseismology studies, however, indicate that earthquakes are non-uniformly distributed in both time and space (*e.g.*, Sykes, 1971; McGuire, 1979; Ma *et al.*, 1989; Shi and Gao, 1991; Working Group, 1988, 1990, 1995; Zhang, 1993). As described in a previous section, the known earthquake distribution across continental Asia deviates from the premise of the seismic source zone. These temporal and spatial variations in seismic potential need to be incorporated in the delineation of seismic source zones in order to realistically assess seismic hazard.

In the conventional method of probabilistic seismic hazard analysis (Cornell, 1968; Algermissen *et al.*, 1976, 1982) the parameters of earthquake activity in a seismic source zone are determined by seismicity statistics, an approach that precludes delineation in enough detail to adequately represent the spatial variation in earthquake distribution. Thus, the statistical rate of earthquake activity might not represent the 'true' future earthquake potential. Also, if an assumed seismic source is larger than any of the zones, its earthquake potential would be averaged across many zones and the probability of

Table II. Annual rate of seismicity at each magnitude interval.

Magnitude interval	Number of sources at the interval	Annual rate at the interval
5.5	15	0.0901
6.3	15	0.0679
6.5	14	0.0066
6.8	12	0.0065
7	9	0.0028
7.2	6	0.0020
7.3	4	0.0008
7.8	3	0.0023
8	2	0.0005
8.5	1	0.0007

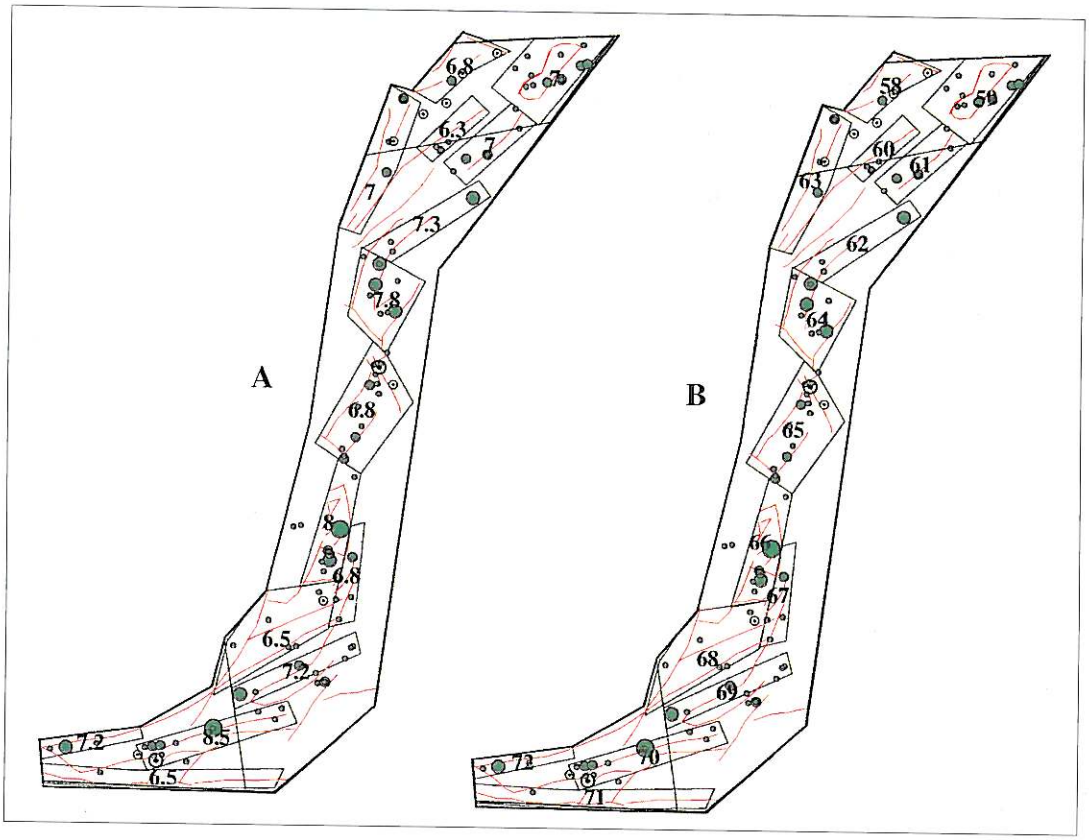

Fig. 5. Example of seismic source delineation within the Shanxi seismic belt. Numbers in A indicate the maximum magnitude earthquake within each source. Numbers in B are the source zone identification numbers.

earthquake recurrence along it might be diminished. To address these possible problems and to reduce the uncertainty in the delineation of seismic source zones, Liu (1987) suggested a two-level delineation of seismic source zones.

The first level of seismic source zone delineation is a seismic belt (or seismic region). The size of a seismic belt is large enough to encompass adequate earthquake data for statistical analysis. Although the seismic belt may include several seismic sources with different characteristics, the rate of earthquake activity within the belt represents the average earthquake potential over the entire seismic belt for the time period of interest. The Shanxi graben seismic belt in China (fig. 5) is a typical example of this level of seismic source zone. Geological structures or patterns of seismicity in the Shanxi seismic belt illustrate that the entire belt behaves as a system geologically as well as seismically. We can use a single frequency-magnitude relationship to describe its earthquake activity. There have been 112 earthquake events with $M_s > 5$ in this seismic belt. The earliest historical earthquake occurred in 780 B.C. The number of events in the Shanxi graben seismic belt is adequate to perform statistical analysis to obtain the annual rate of seismicity and the b value, both necessary to characterize the seismic potential.

The second level of seismic source zone delineation is the delineation of seismic sources within a seismic belt, to better characterize the

temporal and spatial variability of seismic belts and sources (Liu, 1987; State Seismological Bureau, 1992). Seismic sources within the seismic belt may differ from one another in terms of geometry and maximum magnitude earthquake. For example in the Shanxi seismic belt, we have identified 15 potential seismic sources based on geological, geophysical and seismological information (fig. 5). The maximum magnitudes and other parameters of these 15 seismic sources are listed in table III. Earthquakes of $M_S = 8.5$ are assumed to occur only in seismic source 70; earthquakes of M_S between 7.0 and 7.9 may occur in seismic sources 59, 61, 63, 64, 66, 69, 70 and 72. Earthquakes of $M_S < 5.5$ are assumed to occur anywhere in the seismic belt and may be regarded as background seismicity. While each individual source may obey a different magnitude-frequency relationship, they obey a single magnitude-frequency relationship when summed over the entire seismic belt. In this way, we are able to characterize the temporal and spatial variability.

Using this method, we have divided continental Asia into 26 seismic belts (fig. 6). The delineation of seismic belts is based on regional patterns of seismicity, seismotectonics, geological structure, and regional geophysics. The rate of seismicity in each belt is computed according to the statistical method described below. The Pamir, Western Sichuan and Yunnan, Myanmar, Himalayan frontal arc, Southern Tianshan, and Tibetan plateau are the seismic belts with the highest rates of earthquake activity.

We have delineated 425 seismic sources that are distributed through the 26 different seismic belts (fig. 7). Among these seismic sources, 38 have maximum magnitude earthquakes ≥ 8, 192 have maximum magnitude earthquakes between 7.0 and 7.9, 159 have maximum magnitude earthquakes between 6.0 and 6.9, and 36 have maximum magnitude earthquakes between 5.0 and

Table III. Redistribution of annual rate of earthquake activity in the Shanxi seismic belt. Column 1 is source number. The distribution of these sources is shown in fig. 5. Column 2 is maximum earthquake magnitude of each source. Column 3 to column 9 are weighting coefficients at each magnitude interval for each source. Column 10 is the final annual rate of seismicity for each source.

Source No.	M_{max}	5.5.-6.3	6.4-6.5	6.6-6.8	6.9-7	7.1-7.2	7.3	7.4-7.8	7.9-8	8.1-8.5	Nu-final
70	8.5	0.01333	0.0917	0.09722	0.11111	0.14931	0.20779	0.25	0.4167	1	0.0044
66	8	0.01333	0.14726	0.15278	0.16667	0.20486	0.27922	0.33333	0.5833	–	0.0050
64	7.8	0.06039	0.20281	0.20833	0.22222	0.26042	0.35065	0.41667	–	–	0.0092
62	7.3	0.01333	0.07965	0.08333	0.09259	0.11806	0.16234	–	–	–	0.0026
72	7.2	0.01333	0.08568	0.09028	0.10185	0.13368	–	–	–	–	0.0026
69	7.2	0.15451	0.08568	0.09028	0.10185	0.13368	–	–	–	–	0.0122
63	7	0.06039	0.04819	0.05556	0.07407	–	–	–	–	–	0.0050
61	7	0.06039	0.04217	0.04861	0.06481	–	–	–	–	–	0.0049
59	7	0.10745	0.04217	0.04861	0.06481	–	–	–	–	–	0.0081
67	6.8	0.01333	0.03012	0.03472	–	–	–	–	–	–	0.0013
65	6.8	0.15451	0.04217	0.04861	–	–	–	–	–	–	0.0111
58	6.8	0.01333	0.03614	0.04167	–	–	–	–	–	–	0.0014
71	6.5	0.01333	0.03012	–	–	–	–	–	–	–	0.0011
68	6.5	0.10745	0.03614	–	–	–	–	–	–	–	0.0075
60	6.3	0.20157	–	–	–	–	–	–	–	–	0.0137
		1.0000	1.0000	1.0000	1.0000	1.0000	1.0000	1.0000	1.0000	1.0000	0.0901

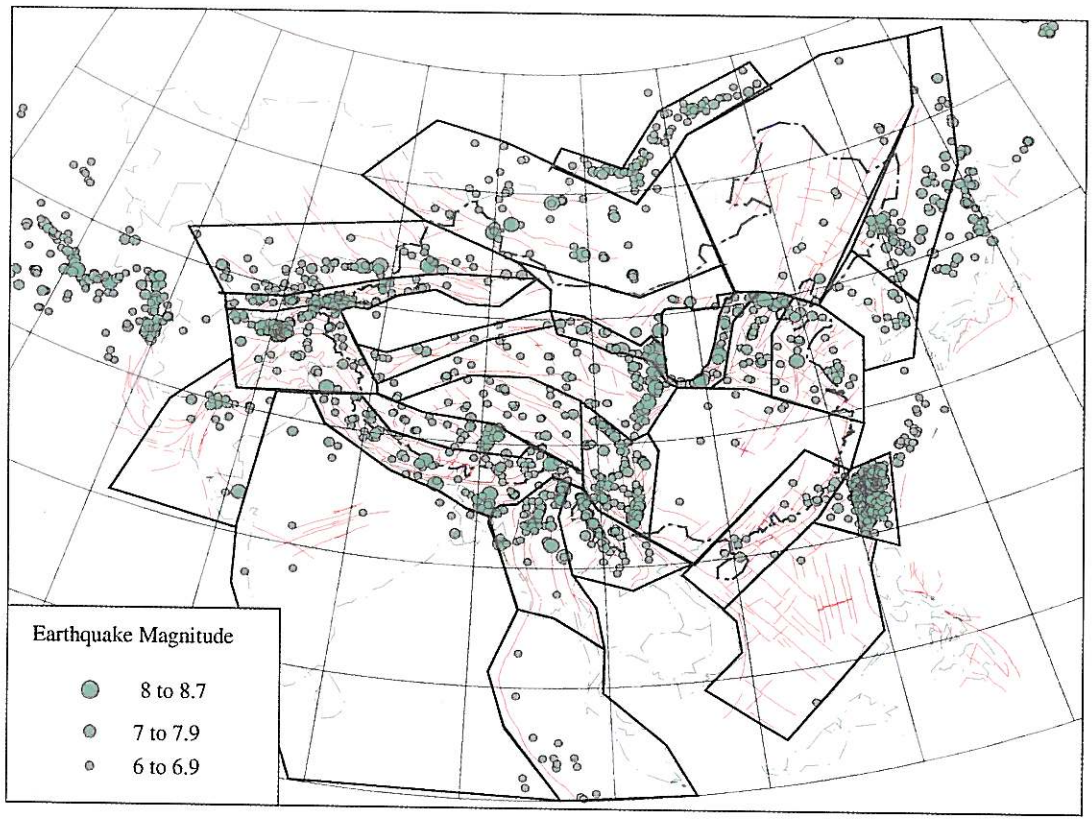

Fig. 6. The seismic source belts (and background source zones) used in the calculation of seismic hazard for continental Asia.

5.9. Most of the seismic sources with the largest maximum magnitude earthquakes are distributed along the Himalayan range front, the Myanmar (Burma) arc, Sichuan and Yunnan, the North China basin, Taiwan, the Tianshan mountains, the Pamir mountains, and the Tibetan plateau. This seismic source distribution coincides with known active tectonic processes as well as the largest historical seismicity.

7. Seismic source zone characterization

The rate of earthquake activity is usually obtained by counting numbers of events with magnitude greater than some lower bound value (called the effective magnitude) within a certain time window. Many factors contribute to the uncertainty in the rate of earthquake activity. The level of completeness of the earthquake catalog for a seismic source has the most impact on the rate uncertainty. Instrumental seismic data provide more precise information for statistical analysis of the rate of earthquake activity, but these data span little more than the previous 30-35 years, which is far less than the average earthquake recurrence interval, especially in intraplate regions. Historical earthquake data span a much longer time period than do instrumental data and provide valuable information on earthquake recurrence. However, the uncertainties in earthquake parameters derived

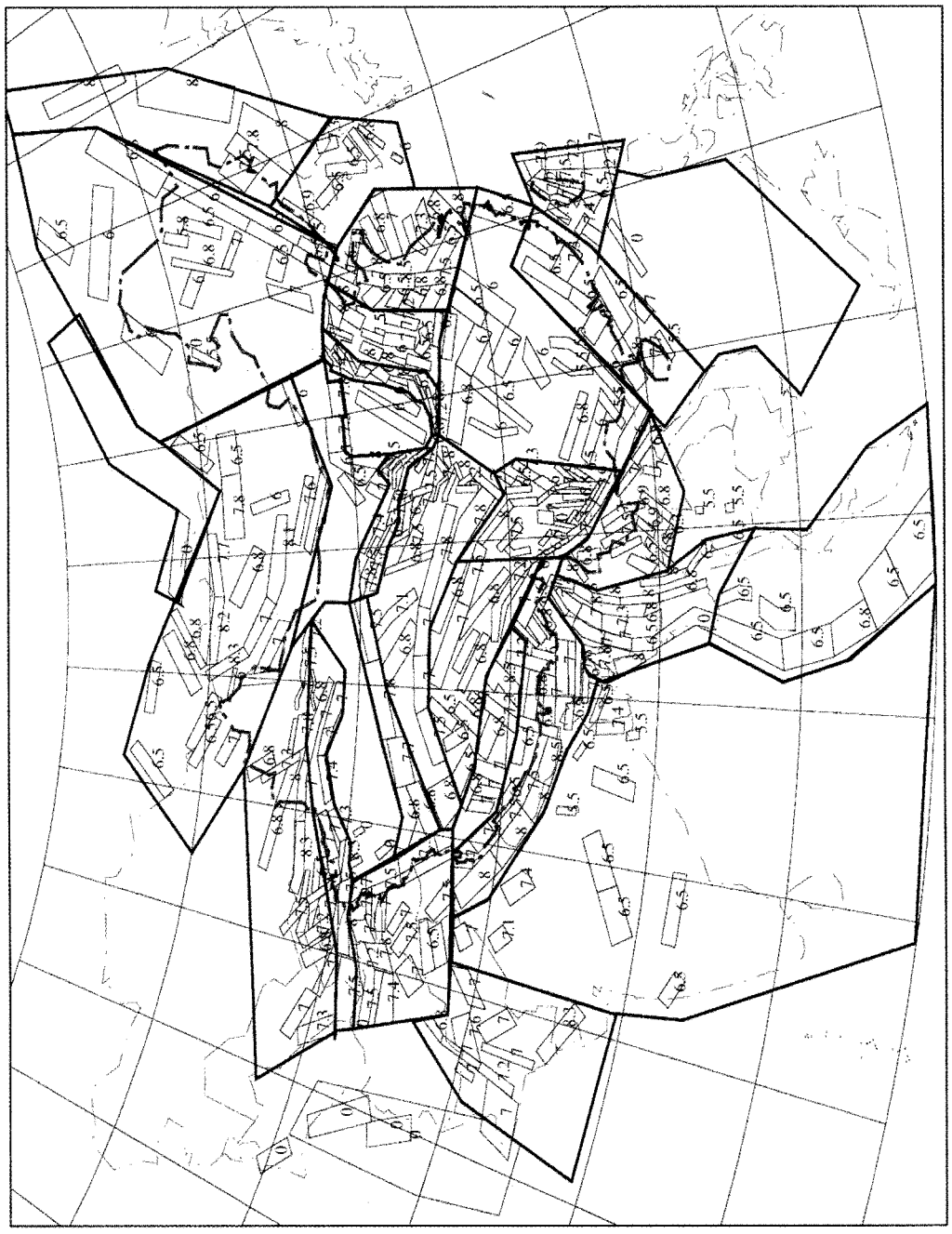

Fig. 7. The seismic sources used in the calculation of seismic hazard for continental Asia.

from historical data are larger than those derived from instrumental data. For example, although the Chinese earthquake catalog covers more than two thousand years, most of the earthquake data in it is limited to general descriptions of earthquake damage, which are subject to interpretation and are far from complete. Thus, one of the critical questions in seismic source characterization is how to combine historical and instrumental data to yield a relatively complete database for statistical analysis of the rate of earthquake activity.

There are two ways to improve the completeness of an earthquake catalog: increasing the number of events listed in the catalog or reducing the time window for statistical analysis. Increasing the number of listed events within a seismic source is unlikely because we cannot alter past earthquake recording history, even though paleoseismology provides some information about large prehistoric events. The length of the statistical time window, however, may be adjusted to improve estimates of parameters based on the completeness of earthquake history. For example, the detection of earthquakes with $M_S \geq 7$ in China may be complete for the past 1000 years because large earthquakes cause significant damages and are likely to be documented as important events. On the other hand, the detection of earthquakes with $M_S = 5$ may be complete for only 200 years or so because smaller earthquakes cause less damage and are less likely to be documented. Thus, it is possible to use different time windows for different magnitude ranges in order to improve parameter estimates based on the completeness levels of earthquake catalogs (Weichert, 1980; McGuire, 1996).

The rate of seismicity in a seismic source belt is distributed to the sources within the belt through the use of weights. A weight is assigned to each seismic source based on careful evaluation and normalization of tectonic activity, number of earthquakes, and number of large earthquakes within each source. In practice, we calculate the annual rate of earthquake occurrence for various magnitude intervals. If there is only one seismic source within a certain interval, such as the one source with a maximum magnitude earthquake = 8.5 in the Shanxi seismic belt (fig. 5), the weight would be one and the entire annual rate of $M_S = 8.5$ earthquakes within the Shanxi seismic belt is assigned to that particular source. If there are several sources within a magnitude interval, we distribute the annual rate of those earthquakes to the sources within that belt according to the assigned weights (Liu, 1987; State Seismological Bureau, 1992; Zhang, 1993). Again using the example of the Shanxi seismic belt, we identified nine maximum magnitude intervals (column 1, table II). Numbers of seismic sources at and above each magnitude interval are listed in column 2 of table I. Column 3 is the annual rate of seismicity in each magnitude interval. The annual rate for earthquakes with $M_S = 8.5$ is 0.0044. Because there is only one source of $M_S = 8.5$ earthquakes within the Shanxi seismic belt, we assign the entire rate (0.0044) to that source. There are six sources with maximum magnitude earthquakes ≥ 7.2. The annual rate for this magnitude interval is 0.0020. The weights of the six sources are 0.118056, 0.260417, 0.204961, 0.133681, 0.149306, and 0.133681 (table III). We multiply the annual rate (0.0020) by these weights to distribute the annual rate to the potential seismic sources (62, 64, 66, 69, 70, and 72 in fig. 5 and table III). We repeat this process for every magnitude interval. Finally, we obtain an annual rate of earthquake occurrence for each seismic source by summing contributions from all possible magnitude intervals below the maximum magnitude interval of each particular source and the background seismicity. Column 12 in table III gives the final rate of earthquake occurrence for the Shanxi seismic belt.

Maximum magnitude is another important parameter in seismic hazard assessment. If the earthquake catalog is long enough within a seismic source zone, the largest historical earthquake can be used as maximum magnitude for the source zone. If the earthquake catalog is not long enough and the potential seismic source is dominated by a single active fault, the fault length or displacement per event determined by paleoseismology results can be used to estimate maximum magnitude (Wells and Coppersmith, 1994). If the seismic source is dominated by multiple faults and the catalog is inadequate, the maximum magnitude estimate from another seismic source with a similar tectonic setting

may be adopted. Fortunately, the test area earthquake catalog is long enough to allow us to use the largest historical earthquake to estimate maximum magnitude for most seismic sources. There are a few seismic sources in the Tibetan plateau where both the catalog and paleoseismology results are inadequate, so we adopted maximum magnitudes from other seismic sources.

8. Strong ground motion attenuation and seismic hazard computation

National seismic hazard maps in most of the countries of the test area depict intensities rather than physical parameters such as peak ground acceleration and peak ground velocity. This is because there is a great deal of descriptive earthquake damage data but only a handful of strong ground motion records (Liu, 1987; Tao and Zheng, 1994). Hu and Zhang (1984) suggested a method to use earthquake intensity data from regions both with and without strong ground motion data to determine strong ground motion attenuation relationships. Using intensity and strong ground motion data from both China and the Western U.S.A., Huo and Hu (1992) determined this strong ground attenuation relationship

$$\ln Y = 0.1497 + 1.9088M - 2.049M^2 -$$

$$- 2.049 \ln [R + 0.1818 \exp (0.7072M)]$$

where Y is the peak ground acceleration at the site. R is the shortest distance (in km) from the site to the vertical projection of the earthquake fault rupture to the surface. M is the surface wave magnitude. This relationship has been widely used in China. We use this relationship for our seismic hazard computation in Asia.

9. Seismic hazard computation

With the exception of Japan and Russia, the seismic hazard values in both the test area and all of continental Asia were calculated using the probabilistic methodology for seismic hazard analysis (Cornell, 1968; Der Kiureghian and Ang, 1975; McGuire, 1976, 1978) as applied by R. McGuire in the program FRISK88M. McGuire (1996) discusses the details of theory, methodology, inputs, and outputs of FRISK88M. Bhatia *et al.* (1999) describe the data and production of the seismic hazard map of India.

The final seismic hazard values for continental Asia were determined using an approach similar to that developed by Frankel *et al.* (1996) for the current U.S. seismic hazard maps. We calculated the seismic hazard posed by two alternative source models and the final map is the weighted average of these results. We first calculated the seismic hazard from the 425 seismic sources. We then calculated the seismic hazard from the 26 seismic belts (or background source zones). We assigned a weight of 0.7 to the hazard from the seismic sources and 0.3 to the hazard from the background source zones. We summed these two maps to produce the final seismic hazard map of continental Asia. The reason for including the background source zones is that earthquakes may occur in areas outside the delineated seismic sources, even though they may not have historically. The inclusion of background source zones lowers the probabilistic ground motions in areas of relatively high historical seismicity while raising the hazard to low levels in areas with no historical seismicity (Frankel *et al.*, 1996). Since the weight for the hazard values from the seismic sources was more than twice the weight for the hazard from the background zones, our inclusion of the hazard from the background zones did not alter the pattern of high and low hazard in continental Asia. The largest reduction (22%) due to the summing occurred in the areas of the highest hazard, but did not remove any of these sites from inclusion in the highest hazard classification.

The tectonic setting of Japan is very complicated. The islands of Japan lie along the eastern edge of the Eurasia plate, which is subducting the Pacific and Philippine plates. Seismicity in and around Japan is driven by the interactions of these plates. Earthquake focal mechanisms indicate that all types of faulting occur, and earthquakes range in depth from the near surface to hundreds of kilometers. Seismic hazard assessment in a region this complicated is a formidable undertaking. The seismic hazard values for

Japan were calculated using the probabilistic method as applied by Annaka and Yashiro (1998). They developed a seismic source model for Japan based on two types of seismic sources: faults that generate large characteristic earthquakes and background sources generating small and moderate earthquakes. They accounted for the temporal variability in earthquake recurrence, and they integrated historical earthquake and active fault data to determine their seismicity parameters. The attenuation relationship for they used was determined especially for Japan by Annaka and Nozawa (1988). Details of their data, methods, and results may be found in several publications (Annaka and Nozawa, 1988; Annaka and Yashiro, 1995, 1998).

The tectonic setting of Russia is primarily intraplate. The most seismically active part of Russia is the Southeastern Kamchatka peninsula, which, like Japan, lies along the eastern edge of the Eurasian plate. The southern border region of Western and Central Russia, including the extensional Lake Baikal region, is also very active seismically. A diffuse area of moderate seismicity northwest of the Kamchatka peninsula aligns with the mid-Atlantic ridge, and is part of the poorly defined Eurasia/North America plate boundary. A few moderate earthquakes also occur along the similarly poorly defined Northern Eurasian plate boundary. A description of the seismic hazard assessment of Russia may be found elsewhere in this volume (Ulomov, 1999).

10. Results

The seismic hazard maps of continental Asia, Japan, India, and Russia (modified) have been combined to form the seismic hazard map of Asia (fig. 8). The seismic hazard map of Asia depicts PGA with a 10% chance of exceedance in 50 years. The site classification is rock. This seismic hazard map of Asia depicts the shaking hazard that will have the largest effect on one to two story structures (the largest class of structures in Asia).

The seismic hazard values for Russia (fig. 8) are modified from the map presented by Ulomov (1999). The seismicity and ground motion attenuation data bases for the Russian map were intensity, rather than magnitude based. All other Asian maps were calculated using magnitude based input data. There is no simple functional equivalence between earthquake intensity values and earthquake magnitudes. Although the use of intensity data to estimate magnitudes is prevalent, the results have large uncertainties (as much as one unit of magnitude) associated with them, especially in intraplate tectonic settings (see Hanks and Johnston, 1992, and Johnston, 1996a,b,c). These uncertainties propagate through the development of attenuation relationships. The intensity based attenuation relationship used to calculate the hazard values for Russia propagates higher ground motions values at all distances than the instrumental magnitude based relationships used elsewhere in Asia. Thus, we have modified the Russian hazard map for inclusion with the rest of Asia by reducing the ground motion attenuation by an average of about 30% at all distances > 20 km. In effect, we have depicted hazard values for Russia that are near the low end of, but within, one standard deviation of those depicted by Ulomov (1999). The values we depict for Russia make the Russian map more consistent with the rest of Asia, and the world. For example, the level of seismicity (rate of earthquake occurrence and probable maximum magnitude earthquake) in the extensional diffuse plate boundary region of Northeastern Russia is much less than that of the extensional North China basin. Our map reflects this, as well as the more gradual ground motion attenuation that occurs in similar crustal structures elsewhere.

The areas of greatest hazard are along the subduction plate boundary regions of the Indian subcontinent, Taiwan, Japan, and the Southern Kamchatka peninsula. The highest hazard values (PGA) in Asia are on Taiwan and along India/Asia collision zone, in Afghanistan, Tajikistan, Nepal, Myanmar, and the Yunnan and Sichuan provinces of China. The widespread deformation associated with the collision of India with Asia is obvious in the hazard map (fig. 8). The entire collision zone is subject to high seismic hazard values (PGA $\geq$ 2.4 m/s^2), and large areas within the collision zone are subject to the highest hazard values depicted (PGA $\geq$ 4.8 m/s^2). The collision of India with Asia is the region

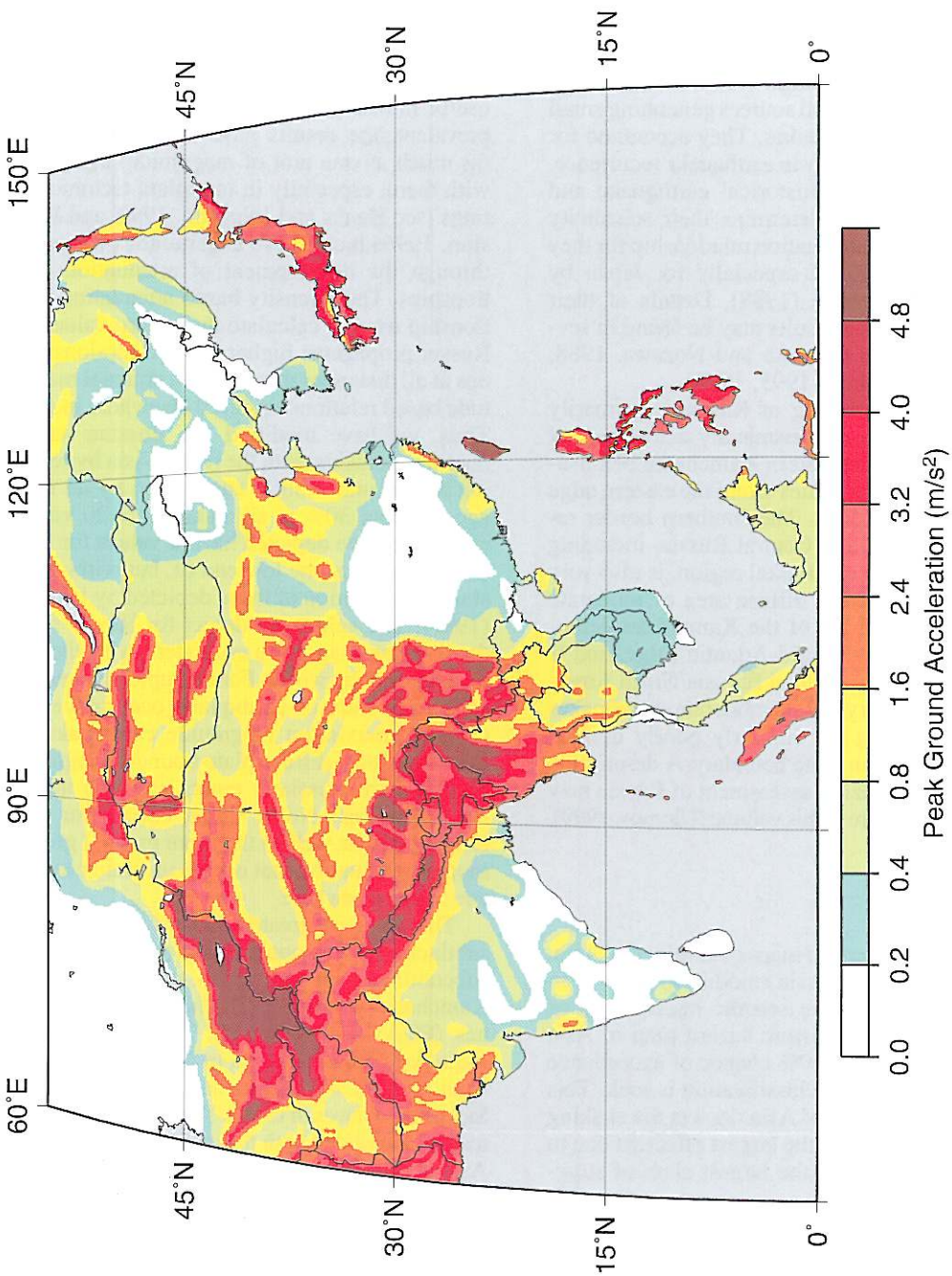

Fig. 8. The seismic hazard map of Asia depicting Peak Ground Acceleration (PGA), given in units of m/s^2, with a 10% chance of exceedance in 50 years. The site classification is rock.

of greatest continental tectonic deformation in the world (Molnar and Deng, 1984; Molnar and Lyon-Caen, 1988; Gupta, 1993). Almost 15% of the great ($M_S \geq 8.0$) earthquakes documented in the twentieth century have occurred here.

The seismic hazard values for Taiwan are all in the highest hazard range (PGA $\geq$ 4.8 m/s^2). Taiwan is the result of the collision between the northern end of an island arc on the Philippine plate and the Eurasian continental shelf (Roecker *et al.*, 1987). South of Taiwan, the Philippine plate is overthrusting the Eurasian plate; east of Taiwan, the Eurasian plate is overthrusting the Philippine plate. The landmass of Taiwan is a product of both plates. The Taiwan Telemetered Seismographic Network (TTSN) records between 4000-5000 earthquakes yearly (Roecker *et al.*, 1987). One of the great ($M_S = 8.0$) earthquakes of the twentieth century occurred on Taiwan in 1920. Thus, it is not surprising that the relatively small island of Taiwan has relatively high seismic hazard values.

Japan, the Kurile Islands, and the eastern Kamchatka peninsula also are areas of high to highest seismic hazard. Twenty percent (20%) of the great ($M_S \geq 8.0$) earthquakes documented in the twentieth century have occurred along this segment of the Pacific/Eurasian plate subduction boundary.

The North China basin, India, and Mongolia contain relatively small areas subject to high levels of seismic hazard. However, the North China basin is the most populous region of China, so the relatively lesser hazard translates into greater risk than in Western China. Northeastern and Southeastern China, most of India, most of Russia, and Southeastern Asia are prone to lower seismic hazard values with respect to other parts of Continental Asia (fig. 8).

The seismic hazard (PGA) values in Asia reflect the complicated regional seismotectonics. The highest hazard values are along the subduction zones that border Eastern and Southwestern Asia.

Acknowledgements

Major contributors for this project are: Peizhen Zhang and Zhi-xian Yang from the China Seismological Bureau; H.K. Gupta and S. Bhatia from the National Geophysical Research Institute of India; K.M. Shedlock from the U.S. Geological Survey; R.M. McGuire from Risk Engineering, Inc., U.S.A.; J.R. Choudhury from the University of Engineering and Technology, Bangladesh; Myint Swe from the Department of Meteorology and Hydrology, Myanmar; A.V. Timush from the Institute of Seismology, Kazakhstan; E.A. Rogozhin from the Joint Institute of Physics of the Earth, Russia; M.R. Pandey from the National Seismological Center, Nepal; N.D. Xuyen from the Institute of Geophysics, Vietnam; Lim Peng Siong from the Geological Survey of Malaysia; Delfin Garcia from the Institute of Volcanology and Seismology, Philippines; Tadashi Annaka from the Tokyo Electric Power Services Company, Japan, and Chang S-N., from the Central Geological Survey, Taiwan.

We thank Domenico Giardini, Peter Basham, and Michael Berry for their help and guidance throughout this project.

REFERENCES

ALGERMISSEN, S.T. and D.M. PERKINS (1976): A probabilistic estimates of maximum acceleration and velocity in rock in the contiguous United States, *U.S. Geol. Surv. Open-File Rep. 76-416.*

ALGERMISSEN, S.T., D.M. PERKINS, P.C. THENHAUS, S.H. HANSON and B.L. BENDER (1982): Probabilistic estimates of maximum acceleration and velocity in rock in the contiguous United States, *U.S. Geol. Surv. Open-File Rep. 82-1033.*

ALI, M.H. and J.R., CHOUDHURY (1994): Assessment of seismic hazard in Bangladesh, in *Proceedings of Workshop on Implementation of Global Seismic Hazard Assessment Program in Central and Southern Asia*, 43-58.

ALLEN, C.R., LUO ZHUOLI, QIAN HONG, WEN XUEZE, ZHOU HUWEI and HUANG WEISHI (1989): Segmentation and rupture history of the Xianshuihe fault, Southwestern China, *U.S. Geol. Surv. Open-File Rep. 89-315*, 10-31.

ANNAKA, T. and Y. NOZAWA (1988): A probabilistic model for seismic hazard estimation in the Kanto district, in *Proceedings 9th World Conference Earthquake Engineering*, vol. 2, 107-112.

ANNAKA, T. and H. YASHIRO (1995): Seismic hazard mapping in Japan: magnitude-frequency relationships and seismic hazards determined from earthquake and active fault data, in *Proceedings 5th International Conference on Seismic Zonation*, France, 309-316.

ANNAKA, T. and H. YASHIRO (1998): A seismic source

model with temporal dependence of large earthquake occurrence for probabilistic seismic hazard assessment in Japan, in *Proceedings Risk Analysis 98* (in press).

ARMIJO, R., P. TAPPONNIER, J.L. MERCIER and T. HAN (1986): Quaternary extension in Southern Tibet: field observations and tectonic implications, *J. Geophys. Res.*, **91**, 13803-13872.

AVOUAC, J.P., P. TAPPONNIER, M. BAI, H. YOU and G. WANG (1993): Active thrusting and folding along the Northern Tianshan and late Cenozoic rotation of the Tarim relative to Dzungaria and Kazakhstan, *J. Geophys. Res.*, **98**, 6755-6804.

BALJINNYAM, I., B.A. BAYASGALAN, B.A., BORISOV, A. CISTERNAS, G.G. DEM'YANOVICH, L., GANBAATAR, V.M. KOCHETKOV, R.A. KURUCHIN, P. MOLNAR, P. HERVE and Y.Y. VASHCHILOV (1993): Ruptures of major earthquakes and active deformation in Mongolia and its surroundings, *Geol. Soc. Am. Mem.*, **181**, 1-8.

BHATIA, S., H.K. GUPTA, RAO CHITRAKAR, ZHANG PEIZHEN and YANG ZHI-XIAN (1997): Seismic hazard map of GSHAP area comprising Eastern Himalaya, North-eastern India, Burmese arc, South China and adjoining regions, *29 IASPEI Assembly*, P386, Thessaloniki, Greece.

BHATIA, S.C., M.R. KUMAR and H.K. GUPTA (1998): A probabilistic seismic hazard map of India and adjoining regions, *Ann. Geofis.*, **42** (6), 1153-1164 (this volume).

BURTMAN, V.S. and P. MOLNAR (1993): Geological and geophysical evidence for deep subduction of continental crust beneath the Pamir, *U.S. Geol. Surv. Special Paper*, **281**.

CHEN, W.P. and P. MOLNAR (1983): Focal depths and fault plane solutions of earthquakes under the Tibetan plateau, *J. Geophys. Res.*, **88**, 1180-1196.

CORNELL, C.A. (1968): Engineering seismic risk analysis, *Bull. Seismol. Soc. Am.*, **58**, 1583-1606.

CURRY, J.R., F.J. EMMEL, D.G. MOORE and R.W. RAITT (1979): Tectonics of the Andaman Sea and Burma, *Am. Assoc. Pet. Geol. Mem.*, **29**, 189-198.

DER KUIREGHIAN, A. and A. H.-S. ANG (1975): A fault rupture model for seismic risk analysis, *Civil Engineering Studies, Structural Research Series*, No. **419**, University of Illinois, Urbana.

EKSTRÖM, G. and A.M. DZIEWONSKI (1988): Evidence of bias in estimations of earthquake size, *Nature*, **332**, 319-323.

FRANKEL, A., C. MUELLER, T. BARNHARD, D. PERKINS, E.V. LEYENDECKER, N. DICKMAN, S. HANSON and M. HOPPER (1996): National seismic hazard maps: documentation June 1996, *U.S. Geol. Surv. Open-File Rep. 96-532*.

GEOLOGICAL SURVEY OF BANGLADESH (1979): *Final Reports by the Committee of Experts on Earthquake Hazard Minimization.*

GIARDINI, D. and P. BASHAM (1993): The Global Seismic Hazard Assessment Program (GSHAP), *Ann. Geofis.*, **36** (3-4), 3-13.

GIARDINI, D. and P. ZHANG (1994): The global seismic hazard assessment program: implementation in Central-Southern Asia, in *Selected Papers of the Second International Conference on Continental Earthquakes* (Seismological Press), 432-437.

GU, GONGXIU (1983): *Earthquake Catalog of China* (Seismological Press).

GUPTA, H.K. (1993): Seismic hazard assessment in the Alpine belt from Iran to Burma, *Ann. Geofis.*, **36** (3-4), 61-82.

GUPTA, H.K. and S.C. BHATIA (1986): Seismicity in the vicinity of of the India and Burma board: evidence for the sinking lithosphere, *J. Geodyn.*, **5**, 379-381.

HANKS, T.C. and A.C. JOHNSTON (1992): Common features of the excitation and propagation of strong ground motion for North American earthquakes, *Bull. Seismol. Soc. Am.*, **82**, 1-23.

HANKS, T.C., and H. KANAMORI (1979): A moment magnitude scale, *J. Geophys. Res.*, **84**, 2348-2350.

HU, YUXIAN and ZHANG MINZHEN (1984): Method of estimating strong ground motion parameters in the regions of lack ground motion recording, *Earthquake Eng. Eng. Vibration*, **4**, 44-53.

HUO, JUNRONG and HU YUXIAN (1992): Study on attenuation laws of ground motion parameters, *Earthquake Eng. Eng. Vibration*, **12**, 1-11.

INSTITUTE OF GEOLOGY, STATE SEISMOLOGICAL BUREAU (1993): Active faults along the Qiliang Shan - Hexi Corridor, China (Seismological Press).

INSTITUTE OF GEOPHYSICS (1991): *Bulletin of Seismological Observations of Chinese Stations*, State Seismological Bureau.

JOHNSTON, A.C. (1996a): Seismic moment assessment of earthquakes in stable continental regions - I. Instrumental seismicity, *Geophys. J. Int.*, **124**, 381-414.

JOHNSTON, A.C. (1996b): Seismic moment assessment of earthquakes in stable continental regions - II. Historical seismicity, *Geophys. J. Int.*, **125**, 639-678.

JOHNSTON, A.C. (1996c): Seismic moment assessment of earthquakes in stable continental regions - III. New Madrid 1811-1812, Charleston, 1886 and Lisbon 1755, *Geophys. J. Int.*, **126**, 314-344.

KHATTRI, K.N. (1992): Seismic hazard in Indian region, edited by H.K. GUPTA, *Curr. Sci.*, special issue 109-116.

LANZHOU INSTITUTE OF SEISMOLOGY AND NINGXIA SEISMOLOGICAL BUREAU (1982): *The 1920 Haiyuan Earthquake* (Seismological Press, Beijing) (in Chinese).

KRISHINA, J. (1992): Seismic zoning maps of India, edited by H.K. GUPTA, *Curr. Sci.*, special issue, 17-23.

LAY, T. and T.C. WALLACE (1995): *Modern Global Seismology* (Academic Press), pp. 521.

LE DAIN, A.Y., P. TAPPONNIER and P. MOLNAr (1984): Active faulting and tectonics of Burma and surroundings, *J. Geophys. Res.*, **89**, 453-472.

LIU, HUIXIANG (1987): On the seismic zoning map of China, in *Proceedings of International Seminar on Seismic Zonation,* 35-42.

MA, XINGYUAN (1989): *Lithospheric Dynamics Atlas of China* (China Cartographic Publishing House, Beijing).

MA, ZONGJIN, FU ZHENGXIANG, ZHANG YINGZHEN, WANG CHENGMIN, ZHANG GUOMIN and LIU DEFU (1989): *Earthquake Prediction: Nine Major Earthquakes in China* (Seismological Press and Springer-Verlag).

MCGUIRE, R.K. (1976): Fortran computer program for seismic risk analysis, *U.S. Geol. Surv. Open-File Rep. 76-67*, 1-90.

MCGUIRE, R.K. (1978): FRISK: a computer program for seismic risk analysis using faults as earthquake sources, *U.S. Geol. Surv. Open-File Rep. 76-67*, 1-90.

MCGUIRE, R.K. (1979): Adequacy of simple probability models for calculating felt-shaking hazard, using the Chinese earthquake catalog, *Bull. Seismol. Soc. Am.*, **69**, 877-892.

MCGUIRE, R.K. (1996): *FRISK88M: User's Manual.*

MIN, ZHIQUN (Chief Editor) (1995): *Chinese Historical Catalog from 230 B.C. to 1911 A.D.* (Seismological Press, Beijing).

MOLNAR, P. and Q. DENG (1984): Faulting associated with large earthquakes and average rate of deformation in Central and Eastern Asia, *J. Geophys. Res.*, **89**, 6203-6227.

MOLNAR, P. and H. LYON-CAEN (1989): Fault plane solutions of earthquakes and active tectonics of the Tibetan plateau and its margins, *Geophys. J. Int.*, **99**, 123-153.

MOLNAR, P. and P. TAPPONNIER (1975): Cenozoic tectonics of Asia: effects of a continental collision, *Science*, **189**, 419-426.

MOLNAR, P. and P. TAPPONNIER (1978): Active tectonics of Tibet, *J. Geophys. Res.*, **83**, 5361-5374.

NELSON, M.R., R. MCCAFFEY and P. MOLNAR (1987): Source parameters for 11 earthquakes in the Tien Shan, Central Asia, determined by *P* and *SH* waveform inversion, *J. Geophys.Res.*, **92**, 12629-12648.

NI, J. and J.E. YORK (1978): Late Cenozoic extension tectonics of the Tibetan plateau, *J. Geophys. Res.*, **83**, 5377-5387.

PELTZER, G. and P. TAPPONNIER (1988): Formation and evolution of strike-slip faults, rifts, and basins during the India – Asia collision: an experimental approach, *J. Geophys. Res.*, **93**, 15085-15117.

RICHTER, C.F. (1958): *Elementary Seismology* (W.H. Freeman, San Francisco).

ROECKER, S.W., Y.H. YEH and Y.B. TSAI (1987): Three-dimensional *P* and *S* wave velocity structures beneath Taiwan: deep structure beneath an arc-continent collision, *J. Geophys. Res.*, **92**, 10547-10570.

SEEBER, L. and J.G. AMBRUSTER (1981): Great detachment of earthquakes along the Himalayan arc and long-term forecasting, *AGU Maurice Ewing Series*, **4**, 259-277.

SHI, Z. and M. GAO (1991): On the rules and methods of seismic zonation of China, in *Proceedings of Fourth International Conference of Seismic Zonation, Stanford, California*, vol. 3, 409-414.

STATE SEISMOLOGICAL BUREAU OF CHINA (1981): *Report on National Seismic Zonation of China* (Seismological Press).

STATE SEISMOLOGICAL BUREAU OF CHINA (1992): *The Third Edition of National Seismic Zonation Map of China* (Seismological Press).

SWE, M. (1994): Reports on the seismic activity in Myanmar and mitigation, in *Proceedings of Workshop on Implementation of Global Seismic Hazard Assessment Program in Central and Southern Asia* (Seismological Press), 59-65.

SYKES, L.R. (1971): Aftershock zones of great earthquakes, seismicity gaps, and earthquake prediction for Alaska and the Aleutians, *J. Geophys. Res.*, **76**, 8021-8041.

TANG, RONGCHAN, HUANG ZUZHI, QIAN HONG, DENG TIANGANG, JIANG LENQIANG, GE PEIJI, LIU SHENGLI, CAO YANGGUO and ZHANG CHENGGUI (1984): On the recent tectonic activity and earthquake of the Xianshuihe fault zone, in *Collection of Papers of the International Symposium on Continental Seismicity and Earthquake Prediction* (Seismological Press, Beijing), 347-363.

TAO, XIAXIN and ZHENG GUANGFEN (1994): Strong ground motion attenuation study in China, in *Proceedings of Workshop on Implementation of Global Seismic Hazard Assessment Program in Central and Southern Asia*, 217-227.

TAPPONNIER, P. and P. MOLNAR (1977): Active faulting and Cenozoic tectonics of China, *J. Geophys. Res.*, **82**, 2905-2930.

TAPPONNIER, P. and P. MOLNAR (1979): Active faulting and Cenozoic tectonics of the Tien Shan, Mongolia, and Baikal region, *J. Geophys. Res.*, **84**, 3425-3459.

TAPPONNIER, P., G. PELTZER, A.Y. LE DAIN, R. ARMIJI and P. COBBOLD (1982): Propagating extrusion tectonics in Asia: new insights from simple experiments with plasticine, *Geology*, **10**, 611-616.

THENHAUS, P.C. (1986): Seismic source zones in probabilistic estimation of the earthquake ground motion hazard: a classification with key issues, in *Workshop on «Probabilistic Seismic Hazard Assessments», U.S. Geol. Surv. Open-File Rep. 86-185*, 53-71.

ULOMOV, V.I., L. SHUMILINA, V. TRIFONOV, T. KRONROD, K. LEVI, N. ZHALKOVSKY, V. IMAEV, A. IVASTCHENKO, V. SMIRNOV, A. GUSEV, S. BALASSANIAN, A. GASSANOV, R. AYZBERG, T. CHELIDZE, A. KURSKEEV, A. TURDUKULOV, A. DRUMYA, S. NEGMATULLAEV, T. ASHIROV, B. PUSTOVITENKO and K. ABDULLABEKOV (1999): Seismic hazard of Northern Eurasia, *Ann. Geofis.*, **42** (6), 1023-1038 (this volume).

UMESH, C. (1992): Seismotectonics of Himalaya, Seismology in India – an overview, *Curr. Sci.*, special ssue, **62**, 40-71.

WEICHERT, D.H. (1980): Estimation of earthquake recurrent parameters for unequal observation periods for different magnitudes, *Bull. Seismol. Soc. Am.*, **70**, 1337-1346.

WELLS, D.L. and K.J. COPPERSMITH (1994): Updated empirical relationships among magnitude, rupture length, rupture area, and surface displacement, *Bull. Seismol. Soc. Am.*, **84**, 974-1002.

WORKING GROUP ON CALIFORNIA EARTHQUAKE PROBABILITIES (1988): Probabilities of large earthquakes occurring in California on the San Andreas fault, *U.S. Geol. Surv. Open-File Rep.*, **88-398**.

WORKING GROUP ON CALIFORNIA EARTHQUAKE PROBABILITIES (1990): Probabilities of large earthquakes in the San Francisco Bay Region, California, *U.S. Geol. Sur. Open-File Rep. 88-398.*

WORKING GROUP ON CALIFORNIA EARTHQUAKE PROBABILITIES (1995): Seismic hazards in Southern California: probable earthquakes, 1994-2024, *Bull. Seismol. Soc. Am.*, **85**, 379-439.

WU, Z., Z. CAO, B. SHENGTO and Q. DENG (1992): *Active Faults in the Central Tibet* (Seismological Press).

XUYEN, N.D. (1994): Status of seismic hazard assessment in Vietnam, in *Proceedings of Workshop on Implementation of Global Seismic Hazard Assessment Program in Central and Southern Asia*, 74-87.

XIE, YUSHUO, CHEN DELI and DING JINREN (1989): *Chinese Earthquake Catalog with Uniform Magnitude from 1900 to 1980* (Seismological Press).

YANG, ZHI-XIAN (1997): GSHAP earthquake catalog of Continental Asia and its Test Area, in *29 IASPEI Assembly, Thessaloniki, Greece,* p. 338.

YANG, ZHI-XIAN and ZHANG PEIZHEN (1996): The basic data of earthquakes and seismicity parameters in South-Asia test area of GSHAP (abstract), *IASPEI Regional Assembly in Asia, Tangshan, China*, p. 305.

ZHANG, PEIZHEN (1993): Seismic hazard assessment in Continental Asia, *Ann. Geofis.*, **36** (3-4), 41-59.

ZHANG, PEIZHEN (1995): Active faulting and seismic hazard assessment, in *Proceedings of International Conference on Active Faulting Aspects in Seismic Hazard Assessment*, 205-212.

ZHANG, PEIZHEN and YANG ZHI-XIAN (1996): Implementation of GSHAP in Central and Southern Asia (abstract), in *IASPEI Regional Assembly in Asia, Tangshan, China*, p. 301.

ZHANG, PEIZHEN and YANG ZHI-XIAN (1997): Implementation of GSHAP in Continental Asia (abstract), in *29 IASPEI Assembly, 386, Thessaloniki, Greece,* p. 339.

ZHANG, W., D. JIAO, P. ZHANG, P. MOLNAR, B.C. BURCHFIEL, Q. DENG, Y. WANG and F. SONG (1987): Displacement along the Haiyuan fault associated with the great 1920 Haiyuan, China, earthquake, *Bull. Seismol. Soc. Am.*, **77**, 117-131.

ZHOU, HUILAN, H.-L. LIU and H. KANAMORI (1983): Source processes of large earthquakes along the Xianshuihe fault in Southwestern China, *Bull. Seismol. Soc. Am.*, **73**, 171-181.